LAPPEENRANTA UNIVERSITY OF TECHNOLOGY
Faculty of Technology
Mechanical Engineering

DEFINING OF THE MATERIAL MODELS FOR STAINLESS STEELS TO BE USED IN FE MODELING

FE MALLINTAMISESSA KÄYTETTÄVIEN RUOSTUMATTOMIEN TERÄSTEN MATERIAALIMALLIEN MÄÄRITTÄMINEN

Mikko Oikamo 22.11.2013

CONTENTS

SYMBOLS AND ABBREVIATIONS

1 THEORY 6
1.1 Mechanical properties of stainless steels 6
1.2 Stress-strain curves 7
1.2.1 Terms used 8
1.3 True stress and strain 11
1.4 Effect of temperature 12
2 TENSILE TESTS 14
2.1 Test specimen 14
2.2 Circumstances of the tests 16
3 FE- ANALYSIS OF THE TENSILE TESTS 17
3.1 Basics of FE- analysis 17
3.2 FE- models 17
3.3 Geometry of the models 19
3.4 Loads and constraints 19
4 RESULTS 20
4.1 Experimental results at room temperature 20
4.2 Experimental results at low temperature 21
4.3 FEM- analysis results 21
4.3.1 FEM results of room temperature tests 22
4.3.2 FEM results of low temperature tests 23
4.4 Reworking of the stress-strain curves for FEM material 23
5 COMPARISON OF THE RESULTS 25
6 CONCLUSIONS 26

REFERENCES……...……...…..27

APPENDICES

SYMBOLS AND ABBREVIATIONS

℃		Celsius
δ	[MPa]	Stress
δ_o	[MPa]	Offset yield strength
δ_{ou}	[MPa]	Upper yield point
δ_{ol}	[MPa]	Lower yield point
δ_p	[MPa]	Proportional limit
δ_t	[MPa]	True Stress
δ_u	[MPa]	Tensile Strength
A	[mm^2]	Current cross-sectional area
A_i	[mm^2]	Original cross-sectional area
d	[mm]	Diameter
ε		Strain
ε_f		Engineering fracture strain
ε_t		True Strain
L	[mm]	Successive value of the length as it changes
L_0	[mm]	Original value of the gage length
L_f	[mm]	Length at fracture
L_i	[mm]	Original length of the gage section
P	[N]	Axial Force
P_{max}	[N]	Highest force reached during the test
$[k]$		Stiffness matrix
$\{U\}$		Vector of nodal displacements
$\{F\}$		Vector of applied nodal forces
FCC		Face Centered Cubic
FEM		Finite Element Method
Femap		Finite Element Modeling And Postprocessing
SFE		Stacking Fault Energy

INTRODUCTION

The aim of this work is to study the results of tensile tests for austenitic stainless steel type 304 and make accurate FE-models according to the results of the tests. Tensile tests were made at Central Research Institute of Structural Material, Prometey at Saint Petersburg and Mariyenburg in Russia. The test specimens for the tensile tests were produced at Lappeenranta University of Technology in a Laboratory of Steel Structures.

In total 4 different tests were made, two with base material specimens and two with transverse butt weld specimens. Each kind of a specimen was tested at room temperature and at low temperature. By comparing the results of room and low temperature tests of similar test specimen we get to study the results of work hardening that affect the austenitic steels at below room temperature.

The produced specimens are to be modeled accurately and then imported for nonlinear FEM- analyzing. Using the data gained from the tensile tests the aim is to get the models work like the specimens did during the tests. By using the analyzed results of the FE-models the aim is to calculate and get the stress-strain curves that correspond to the results acquired from the tensile tests.

1 THEORY

1.1 Mechanical properties of stainless steels

Stainless steels are alloys that consist of at least 10% chromium. These alloys are very resistant to corrosion, making them immune to rust and also often having higher resistance towards high temperature than plain steel. (Dowling 2007, p. 61) It is the passive blocking layer of stainless steels that repairs itself when under influence of oxygen or an oxidizing chemical that prevents corrosion. Resistance to corrosion being the main reason when choosing proper steel for aesthetic reasons. (Euro Inox 2006, p. 23)

Stainless steel type 304, that is used in the study is part of the 300-series, which are termed austenitic stainless steels. 300-series steels contain around 16 to 25% chromium and 6 to 20% nickel. (Kou 1987, p. 369) Nickel has the property to improve corrosion resistance and to stable the face centered cubical (FFC) crystal structure. (Dowling 2007, p. 62) The chemical composition of austenitic stainless steel type 304 is presented in table 1. (Sathiya et al. 2008, p. 144)

Table 1. Base Material chemical composition of austenitic stainless steel type 304.

Element	C	Si	Mn	P	Cr	Ni
%	0.046	0.344	1.31	0.018	17.8	8.28

Element	Co	Mo	As	Pb	Ti	Fe	Co
%	0.078	0.01	0.015	0.0007	0.035	Balance	0.078

Many factors have to be taken in consideration when examining the mechanical properties of the stainless steels. The manufacturers are well aware of the handling of thermomechanical processing and chemical compositions that affect the mechanical properties. This gives a chance to discuss the wanted properties with producers, who expectedly have differences with the mechanical properties of their manufactured stainless steels. The differences are explained with the complicated metallurgy of stainless steels and the big effect of processing. (Euro Inox 2006, p. 20)

1.2 Stress-strain curves

Stress-strain curves show a variety of different behaviors for different materials. Typical stress-strain curve of mild steel is displayed in figure 1. The straight line OA and further straining to point B is the elastic region, which upon the release of the load reverts the specimen to its initial size without causing any deformation. At the point B the specimen starts to yield and from lower yield point C the extension happens at approximately constant load until point D, which is called the plastic flow. After yield point material is both plastic and elastic and the curve slowly decreases until point E, where the failure of the specimen happens. (Chen & Han 1988, p. 7-8)

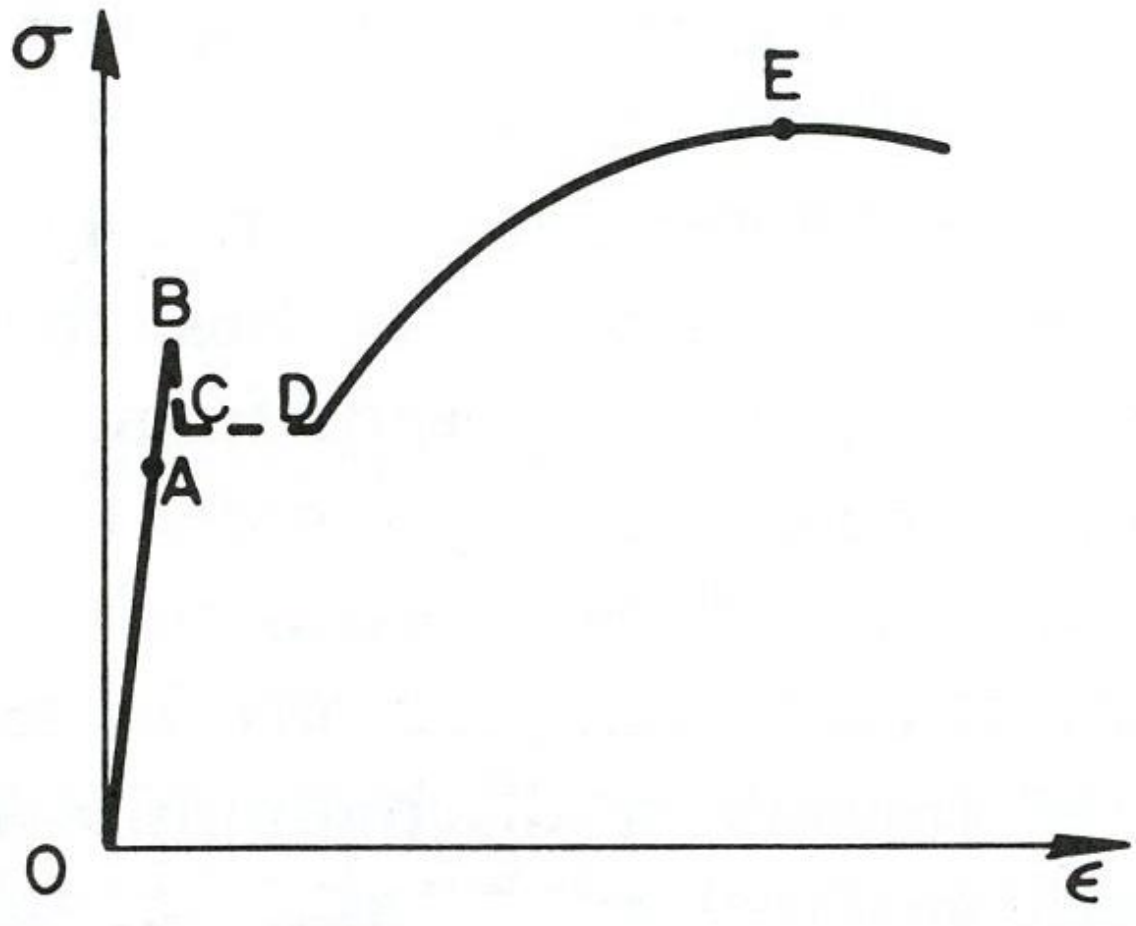

Figure 1. Stress-strain curve for a mild steel. (Adapted from Chen & Han 1988, p. 8)

1.2.1 Terms used

Proportional limit, δ_p, which determines the point where linearity of the stress-strain curve ends does not occur in all materials. Even when linearity is clear, it is still hard to accurately locate where it ends. On this straight line, the elastic modulus, *E*, may be calculated using two points of stresses and strains (Dowling 2007, p. 111, 113):

$$E = \frac{\delta_B - \delta_A}{\varepsilon_B - \varepsilon_A} \qquad [1]$$

where δ is stress

ε is strain

Offset yield strength, δ_o, is used when a yield point can't be precisely defined. Parallel to the elastic slope, *E*, a straight line is drawn, which is normally offset by a standardized strain of 0.2% for engineering metals. In figure 2. there is a stress-strain curve for a typical brittle (a) material where offset yield strength is needed and a stress-strain curve for a typical ductile (b) material where both an upper yield point, δ_{ou}, and lower yield point, δ_{ol}, can be identified. The upper yield point defines where the specimen is no longer able to revert back to its original dimensions, resulting in a permanent deformation. The lower yield point is similar to the offset yield strength and the ability to accurately use it for other stress-strain curves as well, makes it more desirable to be used in general. (Dowling 2007, p. 113)

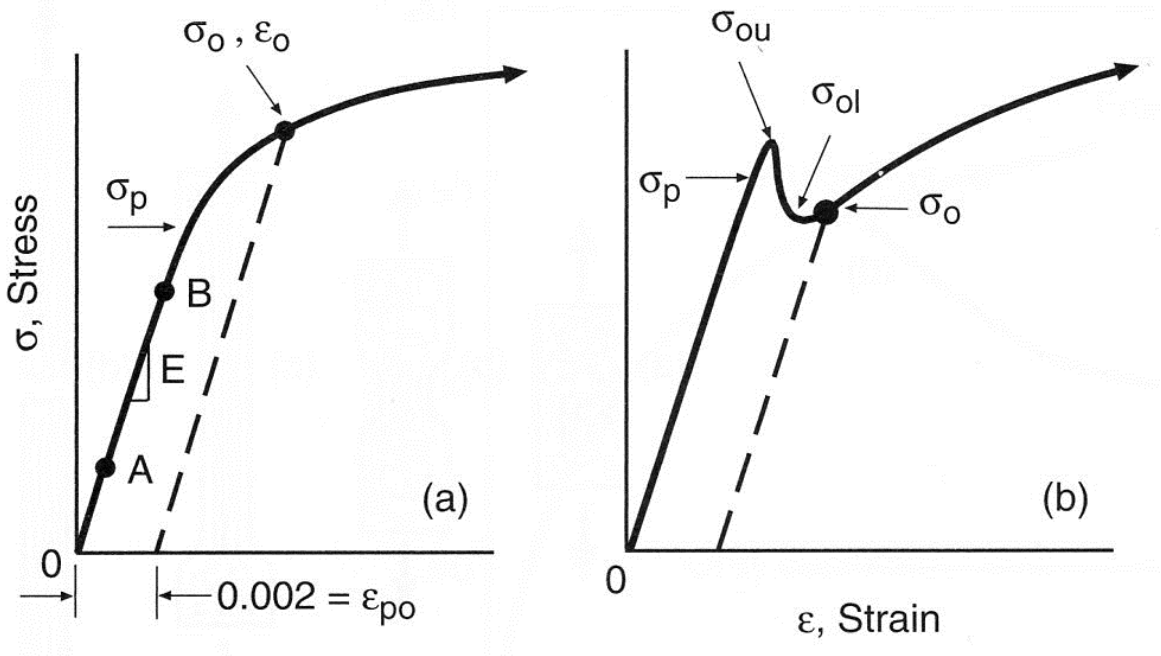

Figure 2. Stress-strain curves for brittle (a) and ductile (b) materials.
(Adapted from Dowling 2007, p. 112)

Tensile strength, δ_u, defines the highest point of stress before the fracture. For brittle behavior the highest stress happens at the point of fracture, which is different from ductile metals that reach the maximum stress before the fracture, so the maximum tensile strength is obtained using (Dowling 2007, p. 112):

$$\delta_u = \frac{P_{max}}{A_i} \qquad [2]$$

where P_{max} is the highest force reached during the test
A_i is the original cross-sectional area

The ability for material to stretch and deform during a tensile test without rupturing is called ductility. The property for specimen to deform elastically is caused by plasticity. One way to define ductility is to get the engineering fracture strain, ε_f, using (Dowling 2007, p. 113-114):

$$\varepsilon_f = \frac{L_f - L_i}{L_i} \qquad [3]$$

where L_f is the length at fracture

L_i is the original length of the gage section

Usual behavior for ductile specimens during a tensile test is necking as presented in figure 3. it means that deformation is centered to a certain area in the specimen, reducing the diameter *d* at that point more than elsewhere. Necking starts to occur when the maximum force is reached, the force diminishing after because of the decreasing cross-sectional area and making the longitudinal strain nonuniform. (Dowling 2007, p. 114)

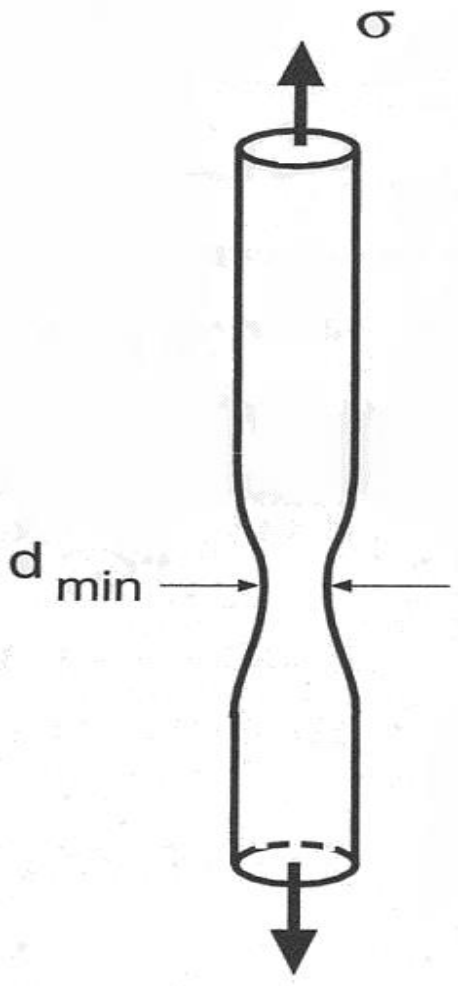

Figure 3. Deformation of a ductile metal during necking.

(Adapted from Dowling 2007, p. 115)

High strain rates happen in both manufacturing and use of the materials, making it the most important parameter to determine the performance in the automotive applications. Austenitic steels have complicated changes during elongation in the microstructural evolution and mechanical behavior for different strain rates and in contrast, the strain rate affects the increase in flow stress for other materials. To understand the overall effect of chemical composition, temperature, stress state and grain size in austenitic steels it is important to figure out how they interact together as it is really helpful when doing FEM simulations. (Talonen 2007, p. 16-17)

1.3 True stress and strain

Engineering stress-strain curves are useful for specimen with small dimensions which are affected by low strains. True stresses and strains differ from engineering stresses and strains, especially with ductile materials, that give a wide difference when plotted into a curve. True stresses and strains are the most appropriate method when analyzing the results of tension tests. True stress δ_t may be calculated either by using the axial force P or the engineering stress δ (Dowling 2007, p. 126):

$$\delta_t = \frac{P}{A}, \qquad [4]$$

$$\delta_t = \delta \frac{A_i}{A} \qquad [5]$$

where A is the current cross-sectional area

The size of cross-sectional area A diminishes during tensile test, resulting in higher stresses than with corresponding engineering stresses. To calculate true strain ε_t, a new stretched gage length is needed (Dowling 2006, p. 127):

$$\varepsilon_t = ln \frac{L}{L_0} \qquad [6]$$

where L is the successive value of the length as it changes
L_0 is the original value of the gage length

The difference with true stress-strain curves compared to engineering stress-strain curves is notable, true stress is always higher compared to engineering stress. Ductile materials for engineering stress-strain curves are affected by necking, resulting in a quick drop in the curve, as for what comes to true stress-strain curves, there is no drop in stress after an ultimate point. This behavior is disabled by using the current area for calculation of the true stress. On the other hand true strain isn't as big as engineering strain unless necking happens, making it significantly larger. (Dowling 2007, p. 131)

1.4 Effect of temperature

Temperature is an important factor for defining the flow stress in addition to strain rate, the reason is the dislocation it sets in motion because of the thermal activation. The increase in temperature results in an increasing thermal activation and also in the decrease of the thermal components of the flow stress. The strain rate is what controls the flow stress, when the strain rate increases, the probability of thermal activation decreases, but the thermal components of the flow stress increase. This is referred to as the positive strain rate sensitivity. (Talonen 2007, p. 17)

In FFC metals yield strength is only slightly affected by temperature and the thermal component of the flow stress is small. FFC metals are though highly affected by stacking fault energy (SFE), which decreases with decreasing temperature, resulting in a possibility that the work-hardening rate of FFC metals increase with decreasing temperature. (Talonen 2007, p.17)

Austenitic stainless steels retain high strength and have an excellent ductility over a wide range of temperatures. The main behavior for both cold-worked and annealed circumstances is that with increasing temperature, the strength decreases. Ductility of austenitic stainless steels being at its best close to a room temperature when it’s least towards very high temperature of few hundred degrees. Work hardening occurs on two occasions at room temperature or below, by decrease for small strains and an increase-

decrease cycle until plastic instability happens. In figure 4. a temperature dependency of engineering stress-strain curves for annealed stainless steel type 304 is displayed. (Byun et al. 2004, p. 3889)

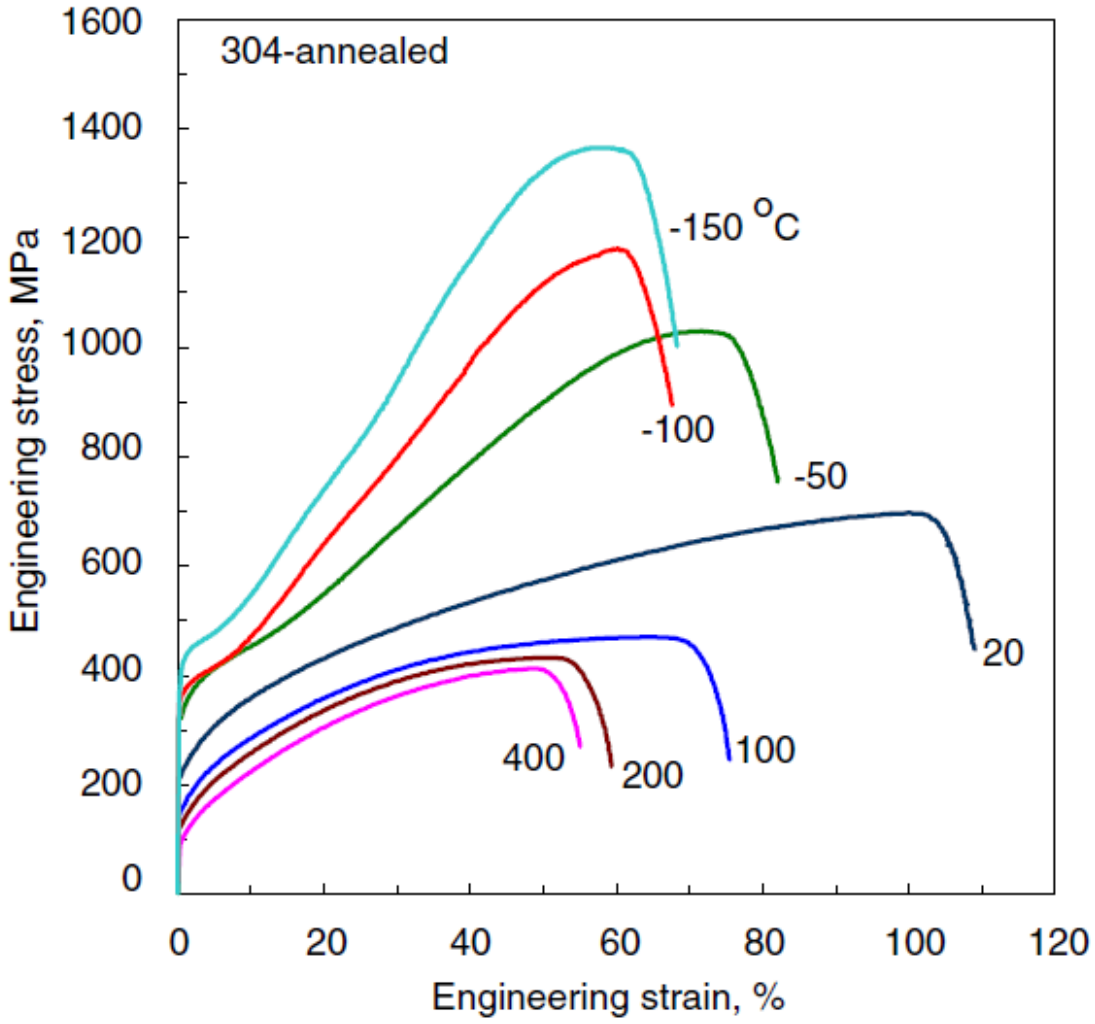

Figure 4. Temperature dependence of the engineering stress-strain curves for annealed 304 stainless teel. (Adapted from Byun et al. 2004, p. 3)

2 TENSILE TESTS

2.1 Test specimen

The test specimens made at Lappeenranta University of Technology in Laboratory of Steel Structures were processed from austenitic stainless steel type 304. In total 4 different tensile tests were made and each was done with 3 identically processed specimens. There were 2 base material specimen tests and 2 transverse butt weld specimen tests. The part to be analyzed is the central part of the specimen with lines drawn to help study the behavior of stainless steel in tensile test. The essential part is the dimensions that are 25 mm wideness and 6 mm thickness. In figure 4. a transverse butt weld specimen is presented for a room temperature tensile test. The weld is 13 mm long and the thickness has been refined to match the steel's, which dimensions are same as the base material specimen's.

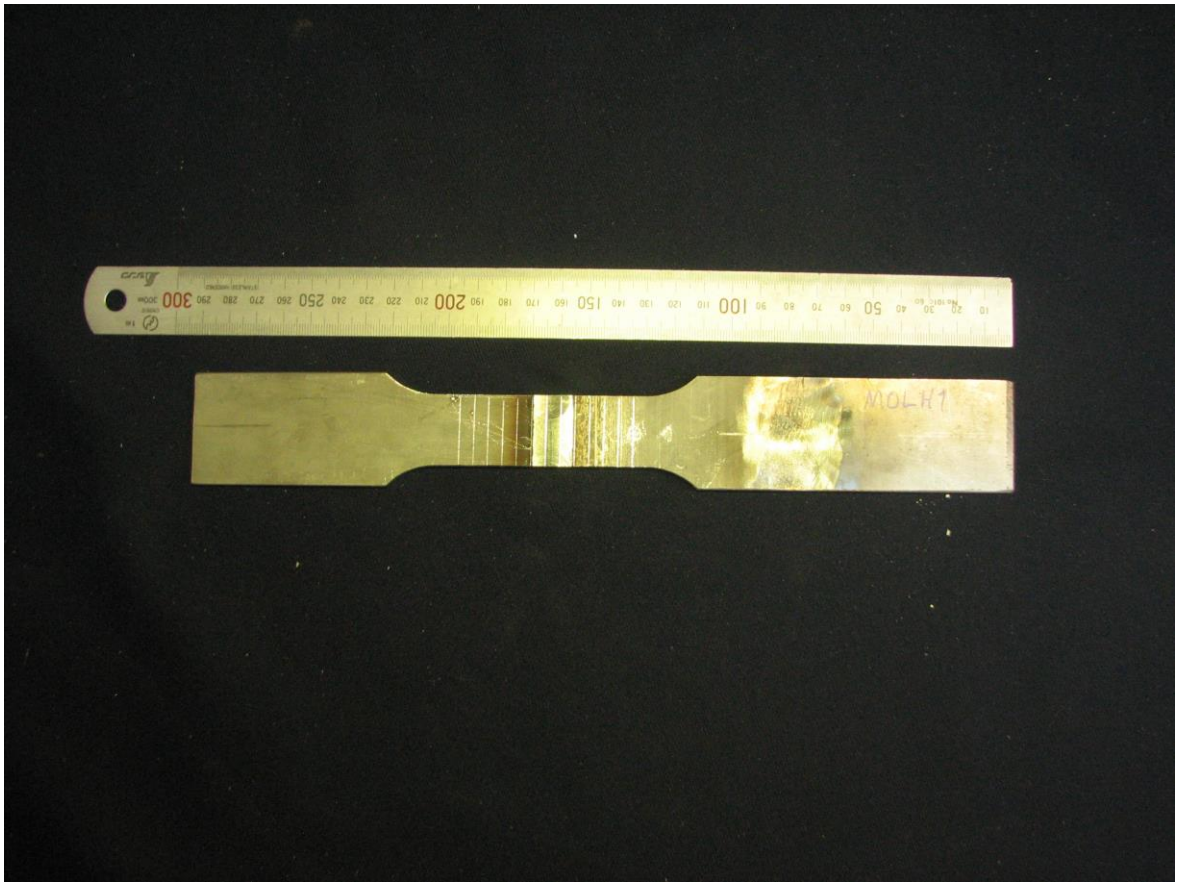

Figure 4. Transverse butt weld specimen for tensile test made at room temperature.

The specimens for low temperature were processed to have large grip sections as shown in figure 5. where a transverse butt weld specimen for low temperature tensile test is presented. The central part of the test piece having the same dimensions as specimens for room temperature tests.

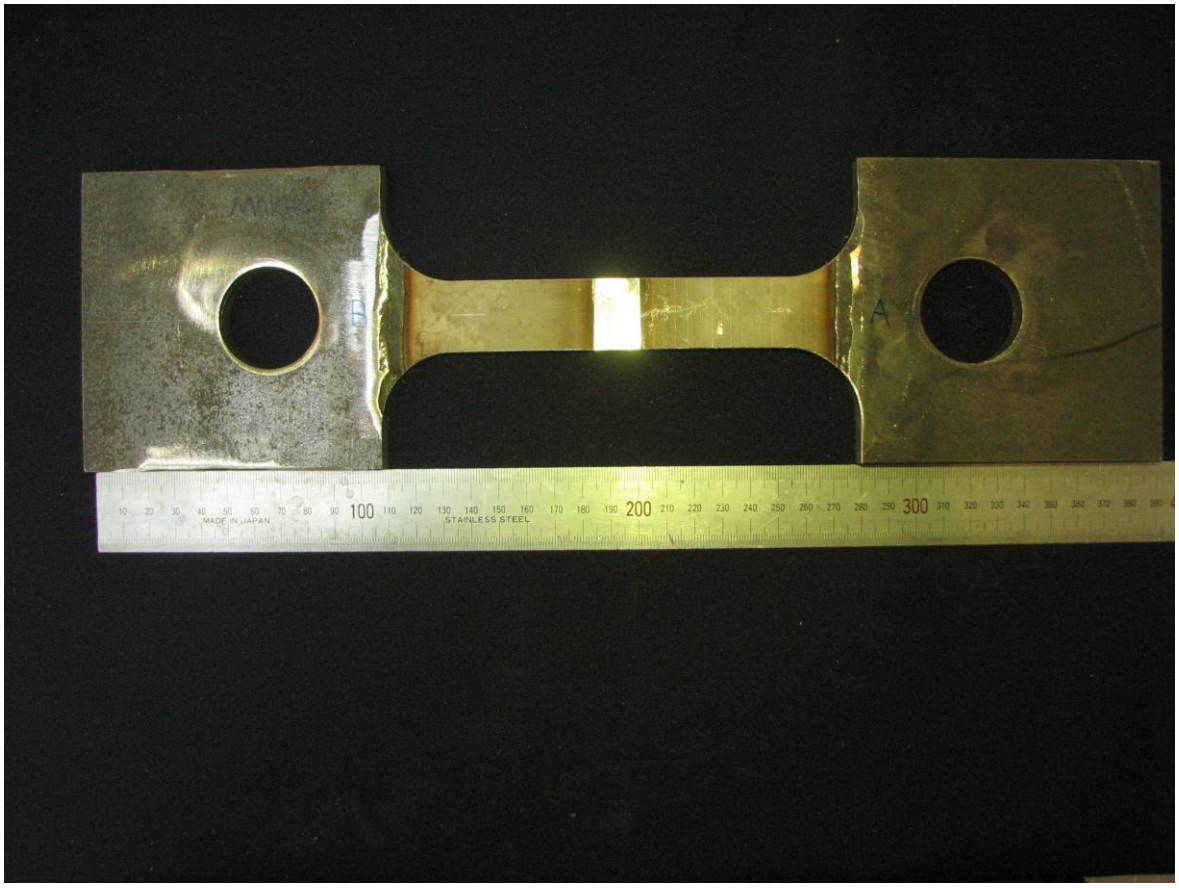

Figure 5. Transverse butt weld specimen for tensile test made at low temperature.

The result of a successful tensile test is shown in figure 6. where the necking has occured especially at the weld before the fracture of the specimen. Fracture itself having happened at the edge of the weld.

Figure 6. Result of a transverse butt weld specimen test made at room temperature.

2.2 Circumstances of the tests

Both base metal specimen and welded specimen were done at room temperature and at low temperature. The tensile tests made at low temperature were done in a cryochamber at a temperature of -46 °C. The test specimens were cooled down to a corresponding temperature using liquid nitrogen and sensors were used to track the temperature for the tests to be made at correct circumstances.

3 FE- ANALYSIS OF THE TENSILE TESTS

3.1 Basics of FE- analysis

FE-analysis is a widely used method to analyze structures, their strength, frequency, tensions and displacements. It is based on an element system, where the structure is divided into small elements that are connected with nodes to help handle even complicated geometries. The more there is elements, the more accurate the results will be. Setting forces and constraints for the nodes allows analyzing the displacement of the nodes, which is used to study the displacement of the entire structure and with using the correct material properties the stresses are acquired. These conditions of the elements are to be changed into the general format. To describe the behavior of the structure the individual element equations are used for the system equations. These are often presented as this function:

$$[k]\{U\} = \{F\} \qquad [7]$$

where $[k]$ is the stiffness matrix
$\{U\}$ is the vector of nodal displacements
$\{F\}$ is the vector of applied nodal forces

For this equation to be solved, constraints for the structure must be defined to prevent unlimited rigid body motion from happening. (Fagan 1992, p. 1, 5-6)

3.2 FE- models

The test specimens made at Lappeenranta University of Technology, were accurately measured before the tensile tests. Test specimens were slightly curved because they were manufactured from pipe. Laser measuring equipment was used to define the shape of the test pieces, which was taken into account when making the models. First step was to make the 3D-models using SolidWorks as displayed in figure 7.

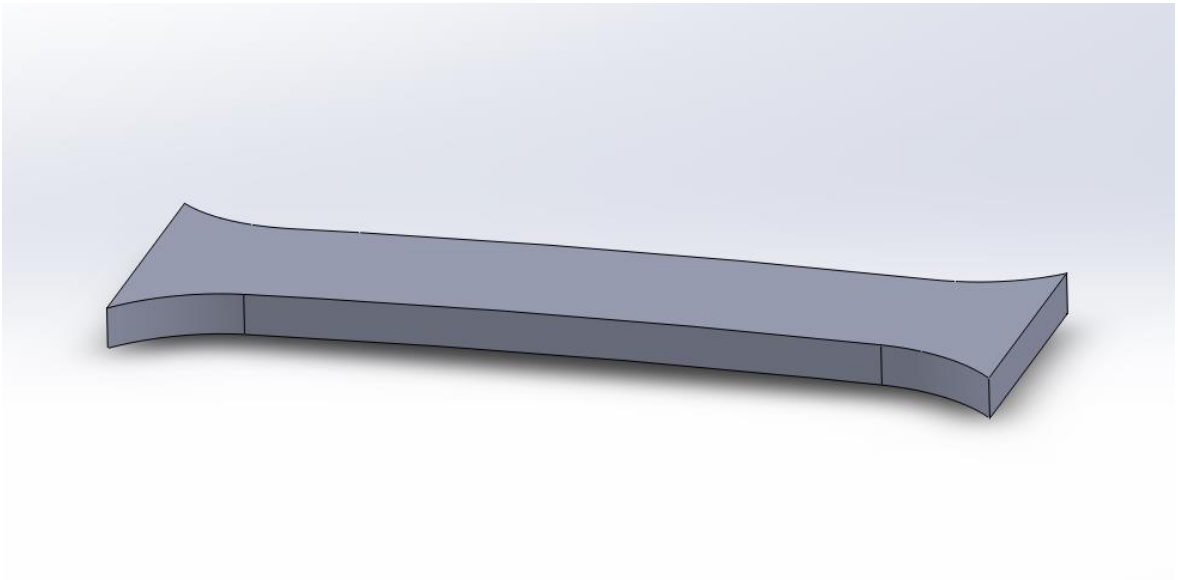

Figure 7. 3D-model of base material specimen.

The 3D-models were then imported to Femap, program used for analyzing the solid models. Models were meshed with tetrahedron elements that had midside nodes, which is a pyramid like 3D-solid element. The reason behind it was to get accurate results. A meshed model for welded specimen is presented in figure 8. For welded specimens, the welding was modeled separately, which is why the meshing isn't totally symmetrical in the model. The reason for this was, that a different material property was used for the weld according to the stress-strain curves acquired from the tensile tests. Then the weld and base material were attached together.

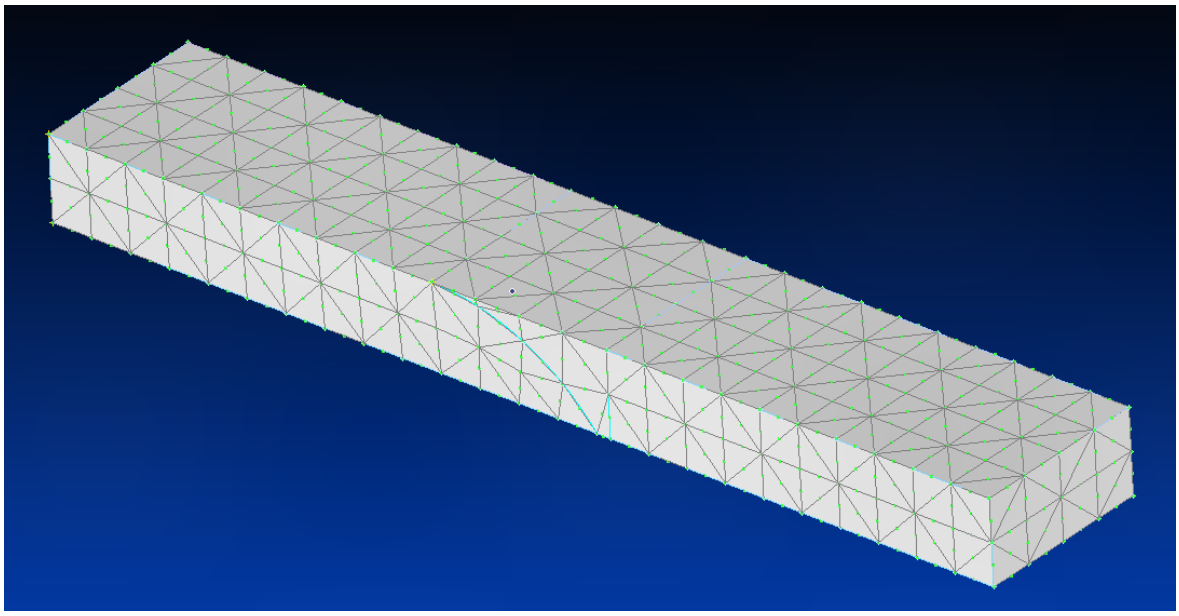

Figure 8. Meshing for a welded model.

3.3 Geometry of the models

Base metal models were reduced to a quarter of their original size, using symmetry as an advantage to reduce the amount of calculations needed and removing the grip sections as they were not an important part of the analysis. Welded models were sliced in half using the symmetry as presented in figure 8. and a different property was made for the welded part of the model, using the data gained from the tensile tests made at Prometey.

3.4 Loads and constraints

Load was put to the nodes on the other end of the model as a displacement which happened to the original gauge length in the tensile tests. Other end of the model was constrained to allow the necking of the specimen.

4 RESULTS

4.1 Experimental results at room temperature

The results from tensile tests included the force and displacement of the specimens at time's function which was turned into stress-strain curves using Excel. A stress-strain curve for base material and welded specimen is displayed in figure 9. These room temperature test pieces were chosen for FE-modeling.

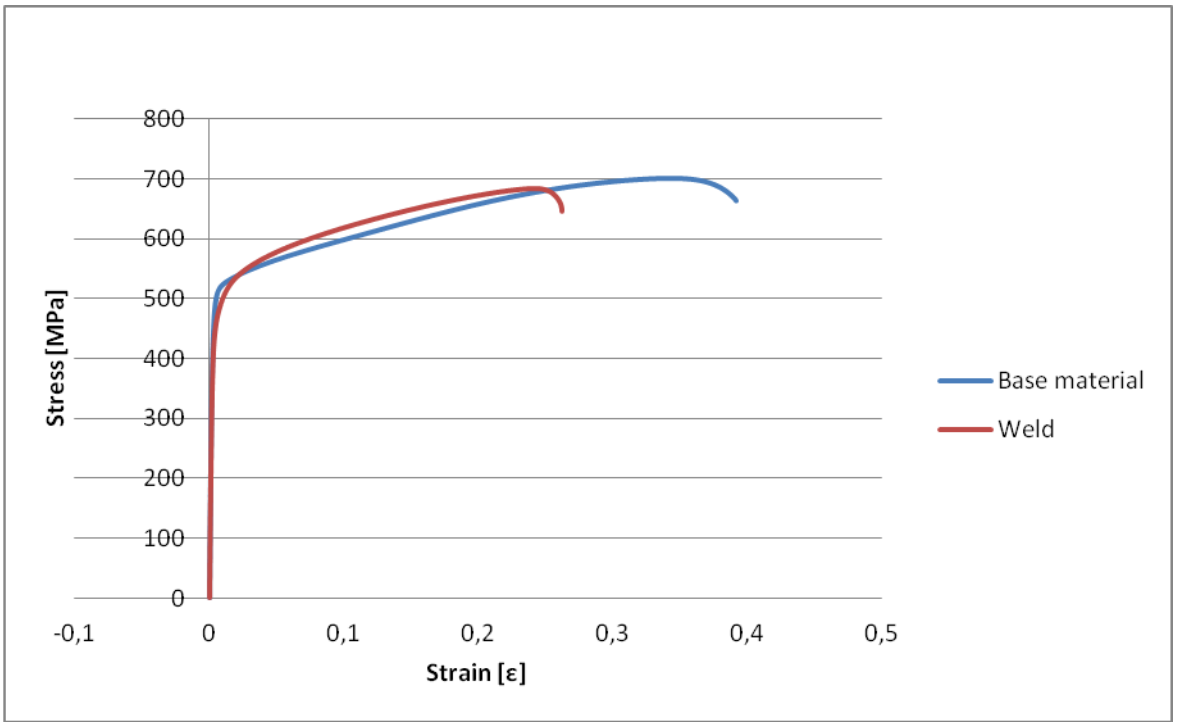

Figure 9. Stress-strain curves for tests made at room temperature.

Figure 9 shows that the stress-strain curve's plastic behaviour is close to each other, but the yield strength is significantly lower for welded specimen. Tensile strength is nearly 700 MPa for both specimen's, but the total strain being nearly half less in welded piece compared to base material before the fraction.

4.2 Experimental results at low temperature

Stress-strain curves acquired from tensile tests made at -46 celsius are presented in figure 10.

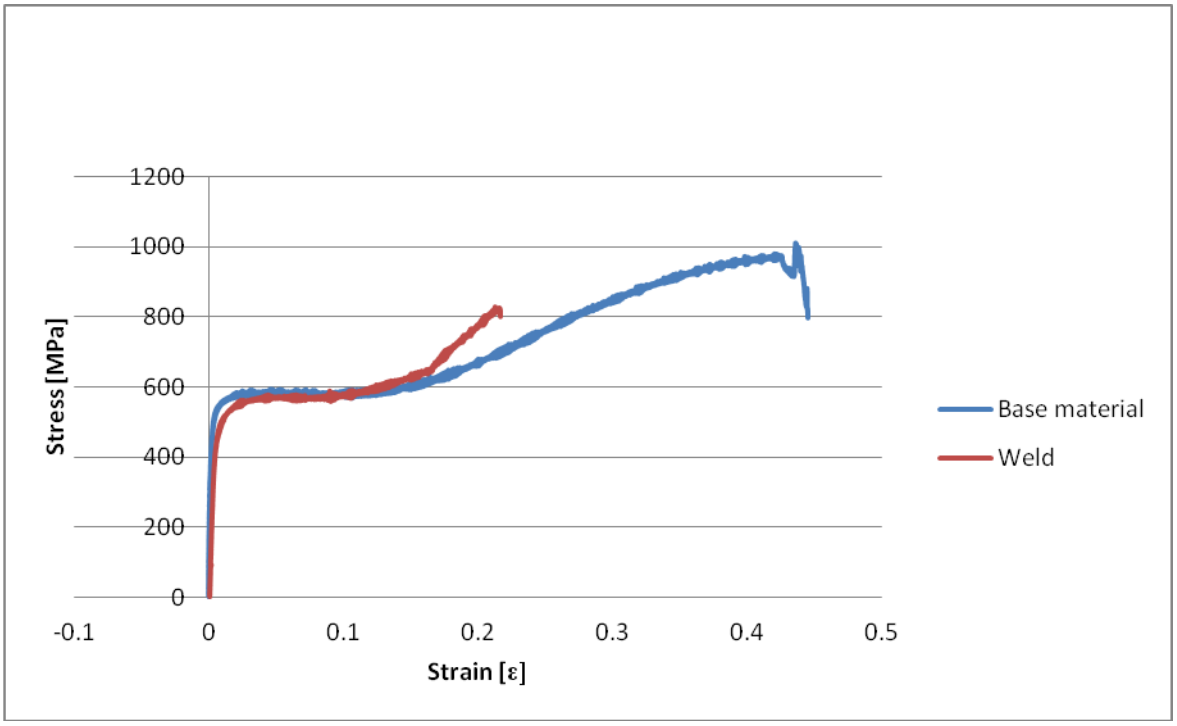

Figure 10. Stress-strain curves for tests made at low temperature.

Firstly the difference between the behaviour of base material and weld is much greater at low temperature than at room temperature. Secondly the difference at maximum stress being over 200 MPa more for base material and the difference in strain before fraction being under half at the welded specimen.

4.3 FEM- analysis results

FEM-analysis were carried out using Femap 10.3.1 engineering analysis program using NX Nastran solver. The structures were studied using nonlinear FEM- analysis, having the material properties for weld and base material from the actual tensile tests. Stress was gained from the analysis by using the formula [2] after summing up the axial force of the nodes at different points of axial translation. Axial translation was used to calculate the

strain by using the formula [3]. These nodes had the displacement as force which happened to the original gauge length of test specimen.

4.3.1 FEM results of room temperature tests

The stress-strain curves for tensile tests and FE-models at room temperature are displayed in figure 11.

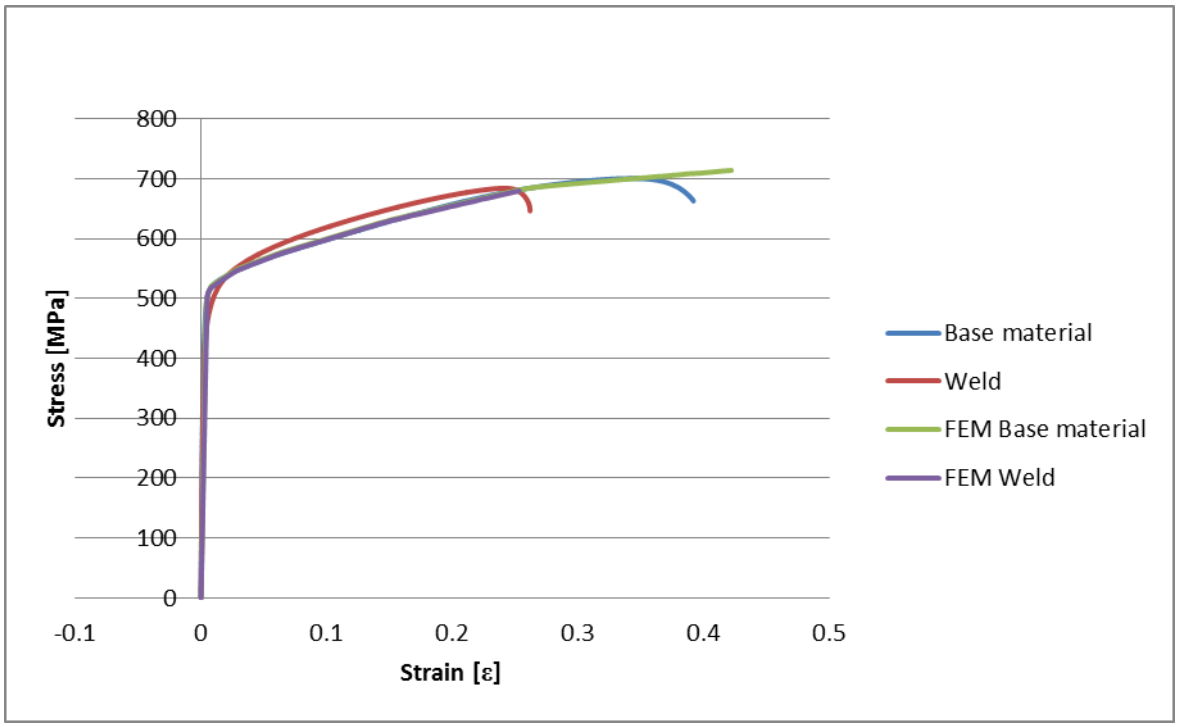

Figure 11. Stress-strain curves at room temperature.

Base material model follows the curve from tensile test nearly perfectly, only that the fracture of the curve does not happen the same way, but that is fine as it is not the important part of this study. As can be seen from the figure 11., the problem with the model with weld is that in the nonlinear analysis the weld does not behaviour as it should and it basicly acts as if the model would consider itself to be only base material.

4.3.2 FEM results of low temperature tests

The stress-strain curves for low temperature tests and FE-models are displayed in figure 12.

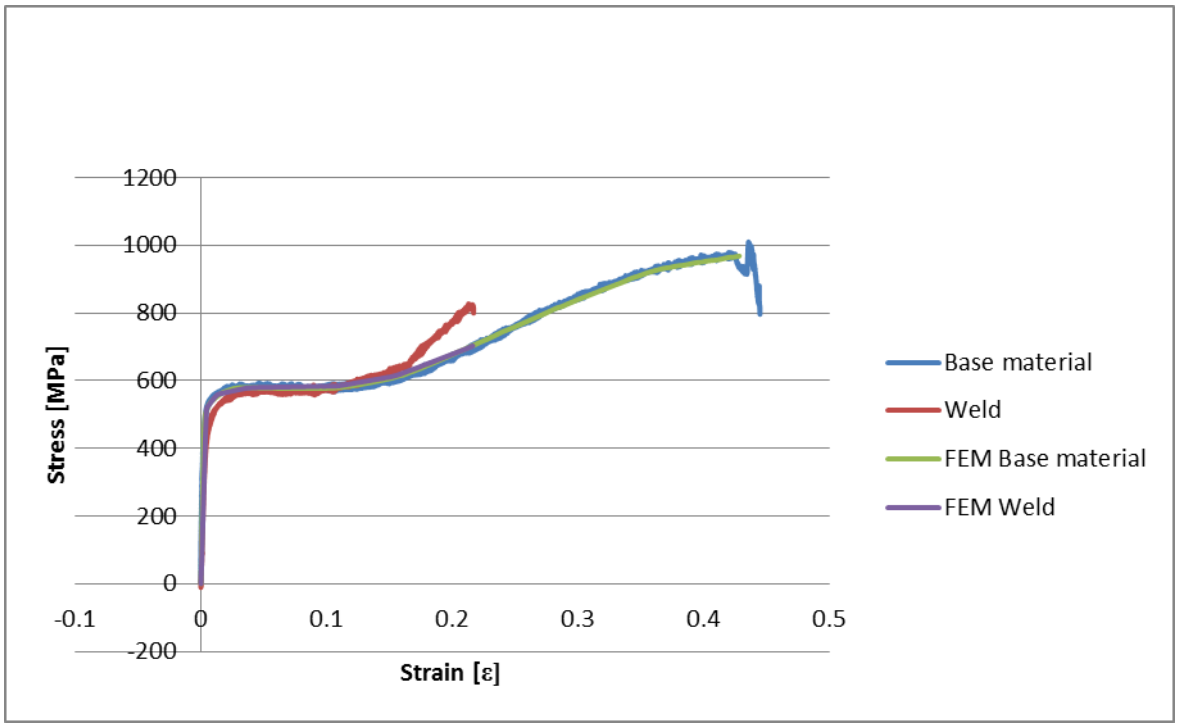

Figure 12. Stress-strain curves at low temperature.

Here we can see the same problem persisting, that the welded model is not behavioring as the test piece. The behaviour is very similar to the base material's until it fractures, this problem will be looked into in chapter 4.4. Base material model is acting like the actual specimen during the tensile test.

4.4 Reworking of the stress-strain curves for FEM material

In order to get the actual behavior of the models to match the tensile tests a change to the strength of weld and base material was needed, this was done by changing the stress-strain function of the materials. The problem was that the necking of the weld didn't happen as it should have and the best solution was to make an overall material function for the whole model. This change made the stress-strain curves for the welded specimens act very similarly as shown in figures 13. and 14.

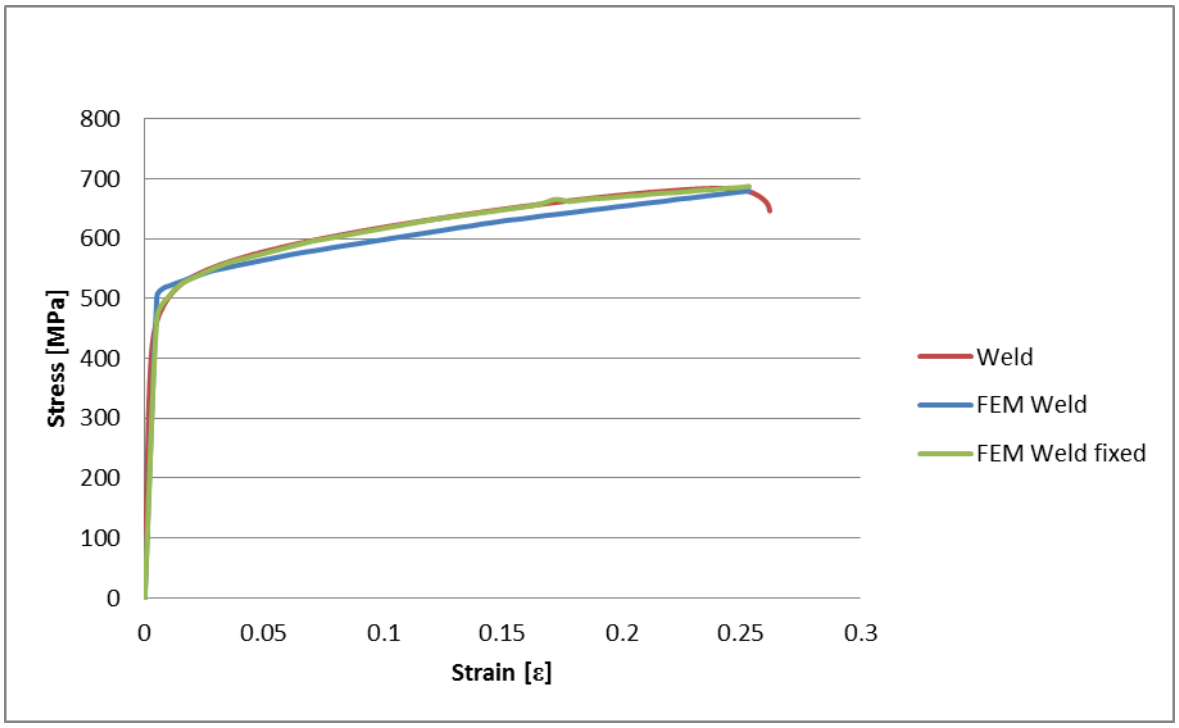

Figure 13. Stress-strain curves for the welded specimen and models at room temperature.

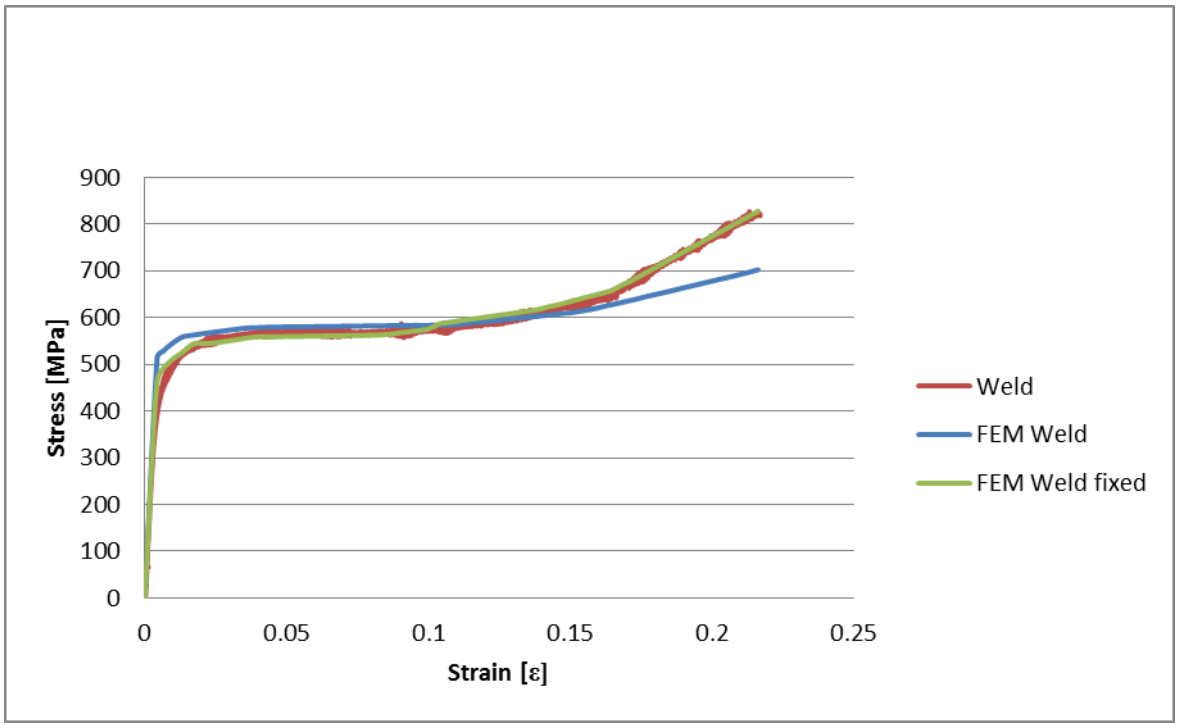

Figure 14. Stress-strain curves for the welded specimen and models at low temperature.

5 COMPARISON OF THE RESULTS

After reworking the stress-strain curves for the welded models, all curves from the tensile tests and FE-models matched each other. The difference between the behavior of the specimen between the room and low temperature tests can be explained with work-hardening that occurs with low temperature tests, strengthening the steel so that it endures higher stress before the fracture, but is less ductile. The results for yield and tensile strength for test specimen are listed in table 1.

	Yield Strength [MPa]	Tensile Strength [MPa]	Max Strain [ε]
Base Material 20 °C	510	700	0.39
Base Material -46 °C	520	971	0.42
Weld 20 °C	460	684	0.26
Weld -46 °C	470	820	0.21

Table 2. Yield and Tensile Strengths with strains of the test specimens.

As can be seen from the table 1, the tests made at low temperature had much higher tensile strength, the difference being 271 MPa for base material and 136 MPa for welded specimen. Yielding happened at roughly the same stress, but the behavior was different at low temperature as the stress did not continuously rise because of the work hardening as it did at room temperature. Strain before the fracture was less at welded specimen by 0.05 ε, which can be explained also because of the work hardening that decreases the ductility of the material. The not expected result is that the strain didn't decrease for base material at low temperature, but increased by 0.03 ε.

6 CONCLUSIONS

The tensile tests made at Prometey were successful and went through as planned. The results from the tests show that the low temperature affected the strength of the specimen, work hardening affecting the test pieces to endure higher stresses before the fracture. It is possible that the ductility of the material did not decrease as an effect of the work hardening because of the behavior of austenitic steel. Temperature being a very dependent factor for the strength of austenitic steel, but the ductility differing between the austenitic steels at different temperatures could explain this.

Elastic properties of austenitic steel can be the factor why the amount of elongation can differ much and many tensile tests would be needed to get approximate results. It can be assumed that if the temperature was lower the difference in engineering strains would be different as the engineering strain would diminish.

FEM –models and properties that were done according to the data from the tensile tests had very similar results when analyzed with Femap. The problem with Femap was to get the necking work as intended, particularly at the weld in the welded models. This didn't work because the base material property made the model work as it was plain base material. Trying to approach the matter by weakening the weld's properties didn't solve the problem, but using the same overall property made the stress-strain curves of analyzed models act like the actual tensile tests. This simplification of the model resulted in weld not acting differently from the rest of the model, but it fixed the ductile behavior so the model allowed necking as it happened in the tensile tests.

REFERENCES

Byun, T. S., Hashimoto, N., Farrell, K., 2004. Temperature dependence of strain hardening and plastic instability behaviors in austenitic stainless steels. Oak Ridge, USA, 2004. Acta Materialia, vol. 52. p. 3889-3899

Chen, W. F., Han, D. J., 1988. Plasticity for structural engineers. New York: Springer-Verlag. 606 p. ISBN 0-387-96711-7.

Dowling, N. E., 2007. Mechanical behavior of materials. Engineering Methods for Deformation, Fracture, and Fatigue. 3. Edition. Upper Saddle River, New Jersey: Pearson Prentice Hall. 912 p. ISBN 0–13–186312–6.

Euro Inox, 2006. Ruostumattomien terästen käyttö kantavissa rakenteissa. Finnish translation from book: Design Manual For Structural Stainless Steel. Brussels. 197 p. ISBN 2–87997–043-1

Fagan, M. J., 1992. Finite Element Analysis. Theory and practice. Harlow: Longman. 315 p. ISBN 0-582-02247-9.

Kou, S., Welding metallurgy. New York: John Wiley & Sons, Inc., 1987. 411 s. ISBN 0-471-84090-4

Sathiya, P., Aravindan, S., Noorul Haq, A., 2007. Tensile properties of similar AISI 304 austenitic and AISI 430 ferritic stainless steels joined by friction welding. India. Multidiscipline Modeling in Mat. and Str. vol 4. p. 141-154.

Talonen, J., 2007. Effect of strain-induced α'-martensite transformation on mechanical properties of metastable austenitic stainless steels. Helsinki University of Technology. [Online] Available at: <http://lib.tkk.fi/Diss/2007/isbn9789512287802/isbn9789512287802.pdf> [Accessed 4 May 2012]

APPENDIX 1. General information of 304 steel and other grades for RHS from Stalatube Oy.

GENERAL INFORMATION

CHEMICAL COMPOSITION											
Austenitic											
(FULFILS THE STANDARDS ASTM A554-11 AND EN 10088-2)											
EN	**MT**	**C %, max**	**Mn %, max**	**P %, max**	**Ni %**	**Cr %**	**Mo %**	**Ti %**			
1.4301	304	0.07	2.00	0.04	8.0-10.5	18.0-19.5	-	-			
1.4307	304L	0.03	2.00	0.04	8.0-10.5	18.0-19.5	-	-			
1.4404	316L	0.03	2.00	0.04	10.0-13.0	16.5-18.0	2.0-2.5	-			
1.4571	316Ti (*)	0.08	2.00	0.045	10.0-13.5	16.5-18.0	2.0-2.5	5x(C+N)-0.7			
For all grades S max 0.015, Si max 0.75 and N max 0.10											
* Fulfils the standards A240-09a and EN 10088-2											
Lean Duplex											
EN	**UNS**	**C % max**	**Mn %**	**P % max**	**Ni %**	**Cr %**	**Mo %**	**Si % max**	**S % max**	**N %**	**Cu %**
1.4162	S32101	0.04	4.0-6.0	0.04	1.35-1.70	21.0 -22.0	0.1-0.8	1.00	0.03	0.2-0.25	0.1-0.8

Also other Duplex grades may be possible on request

MECHANICAL PROPERTIES				
(MEASURED FROM COIL ACCORDING TO EN 10088-2)				
EN	**MT or UNS**	**Yield strenght Rp0.2 min N/mm² (ksi)**	**Tensile strength Rm min N/mm² (ksi)**	**Elongation min %**
Austenitic				
1.4301	304	230 (33)	540 (78)	45
1.4307	304L	220 (32)	520 (75)	45
1.4404	316L	240 (34)	530 (76)	40
1.4571	316Ti	240 (34)	540 (76)	40
Lean Duplex				
1.4162	S32101	480 (70)	680 (98)	30

INSPECTION CERTIFICATE
EN 10204 – 3.1

We reserve the right to changes. Stalatube takes no responsibility for any error in numerical information that might appear in this brochure.

Latest version www.stalatube.com

APPENDIX 2. Results of the room temperature tests.

Zwick / Roell Z250 **Tensile testing**

Испытание на растяжение

Заказ
Отдел
Тема

Заказчик
Рабочий журнал №:
Сстр. :

Результаты:

№	Маркировка	a_0 mm	b_0 mm	L_c mm	E MPa	R_m ($\sigma_в$) MPa	R_{p02} ($\sigma_{0.2}$) MPa	A (δ_5) %	$\delta_{равн\ п}$ %	Примечания
1	MOLP1	5.88	24.91	90	158769	700.4	479.9	53.9	44.1	
2	MOLP2	5.87	24.96	90	174147	694.9	479.7	55.6	45.4	
3	MOLP3	5.86	24.99	90	183338	699.0	480.5	55.0	45.5	
4	MOLH1	5.88	24.86	75	182055	684.1	446.7	29.0	25.9	разрыв по шву
5	MOLH2	5.87	24.62	75	189291	641.1	453.6	16.1	13.1	разрыв по шву
6	MOLH3	5.82	24.86	75	186838	689.7	454.8	26.4	24.0	разрыв по шву

Исполнитель :

Zwick / Roell Z250 Испытание на растяжение

Маркировка: MOLP1

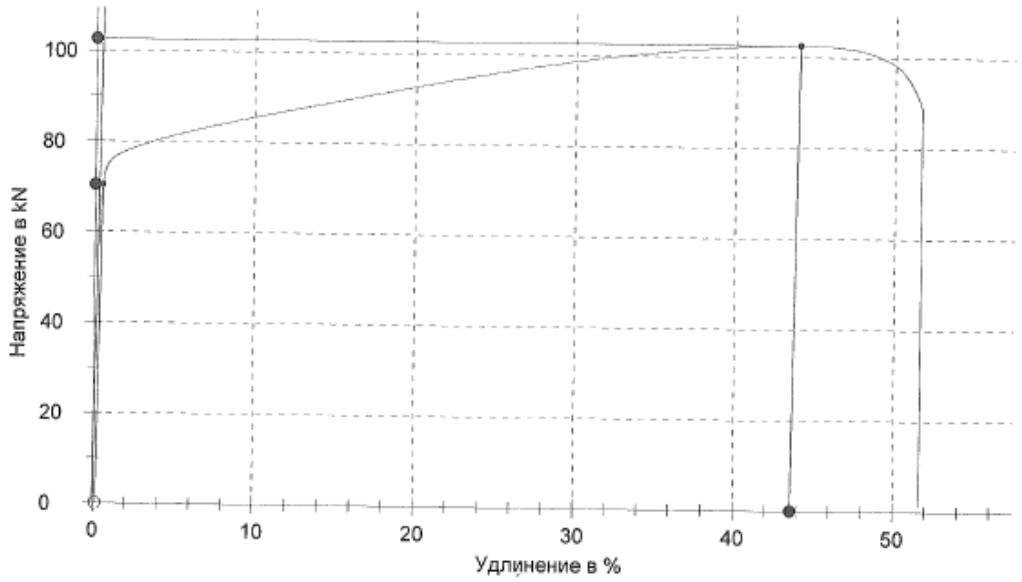

Маркировка: MOLP2

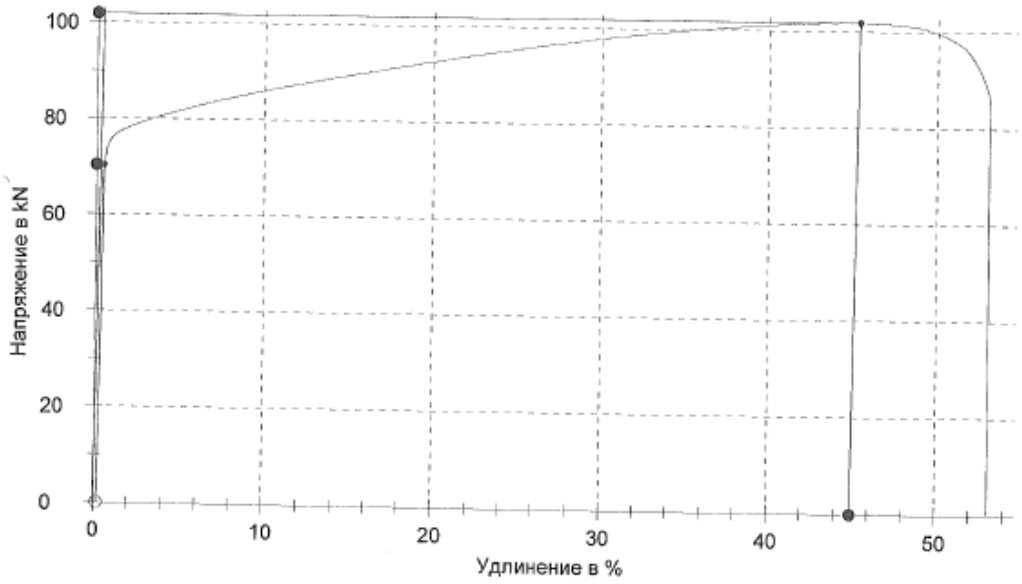

Маркировка: MOLP3

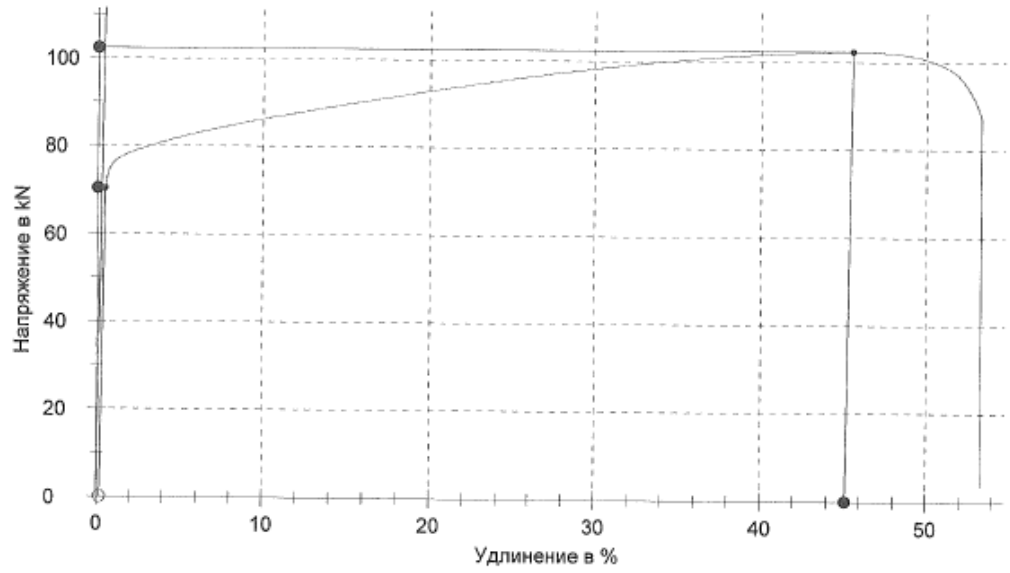

Маркировка: MOLH1

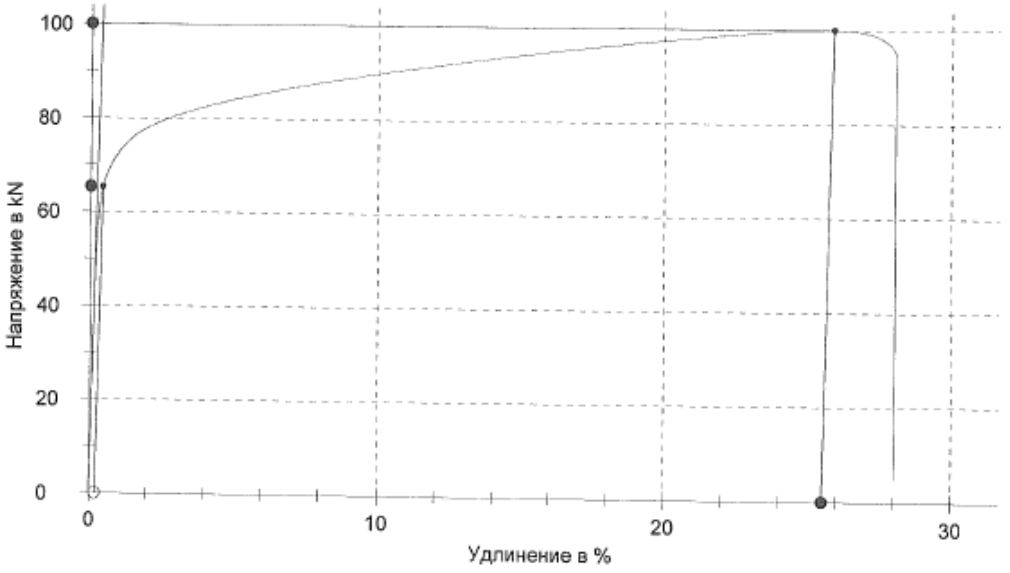

Zwick / Roell Z250 Испытание на растяжение

Маркировка: MOLH2

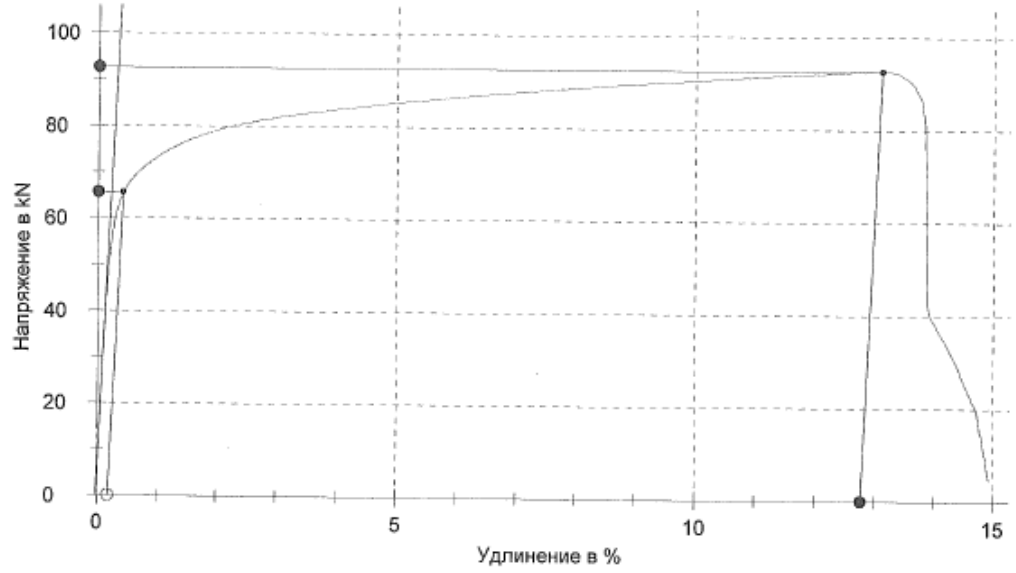

Маркировка: MOLH3

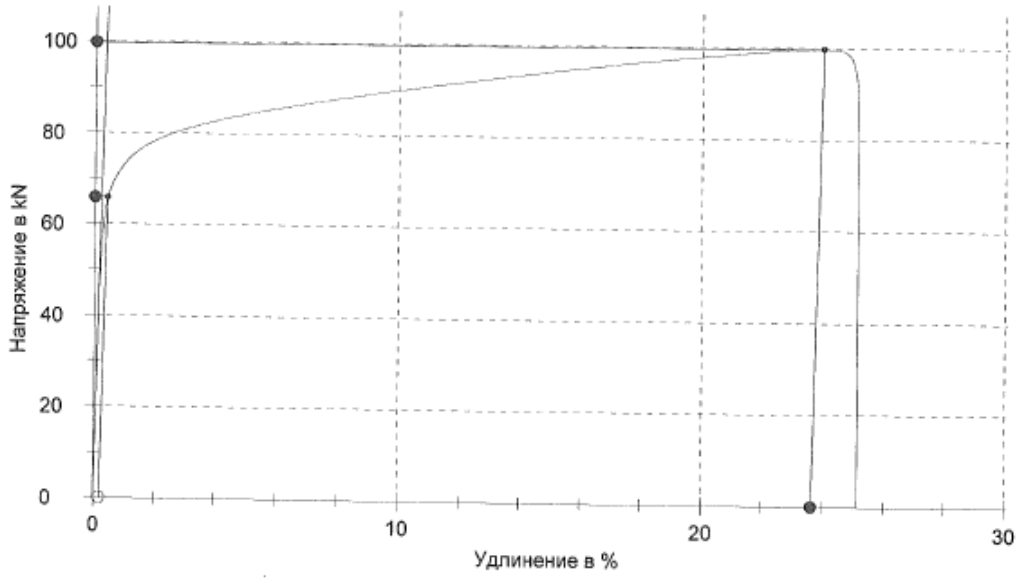

APPENDIX 3. Results of the low temperature tensile tests.

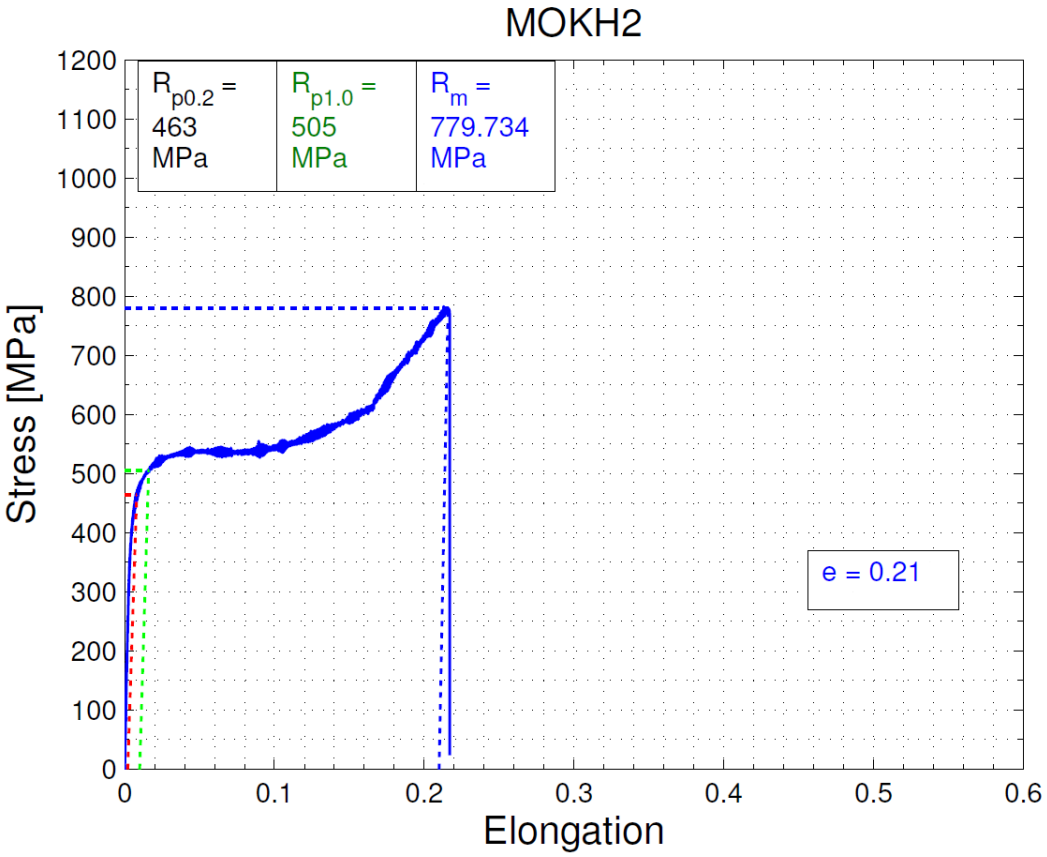

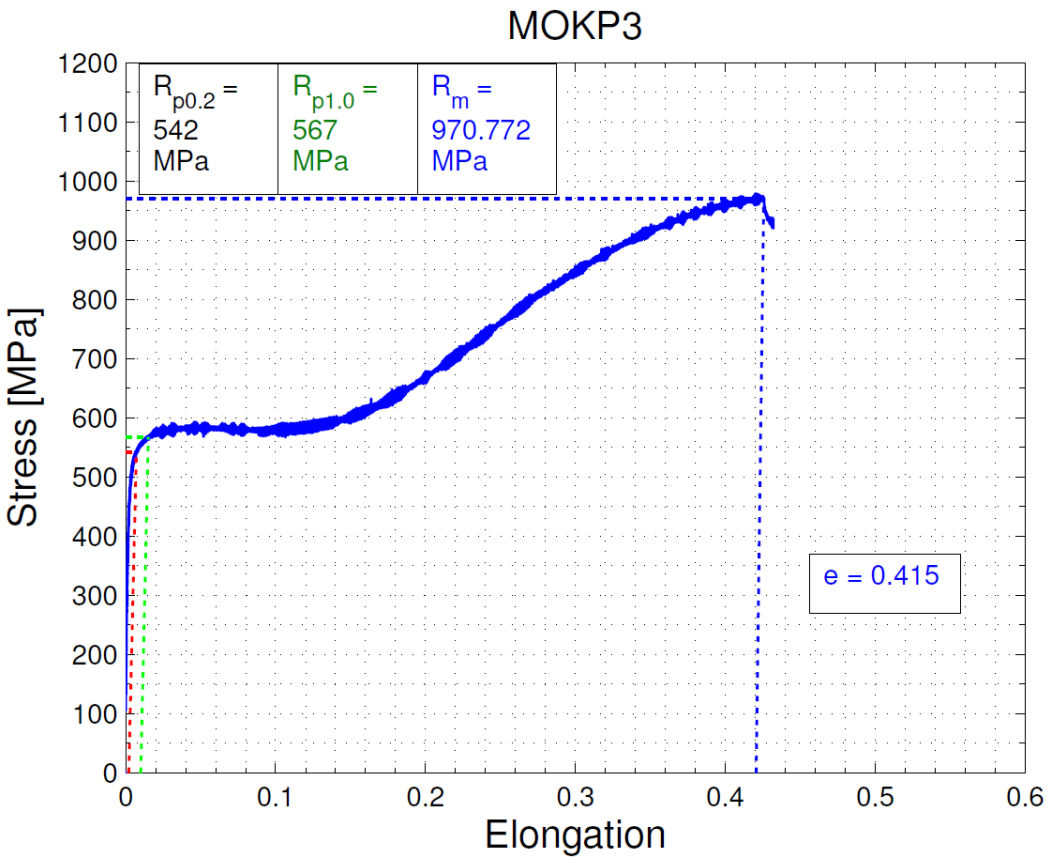
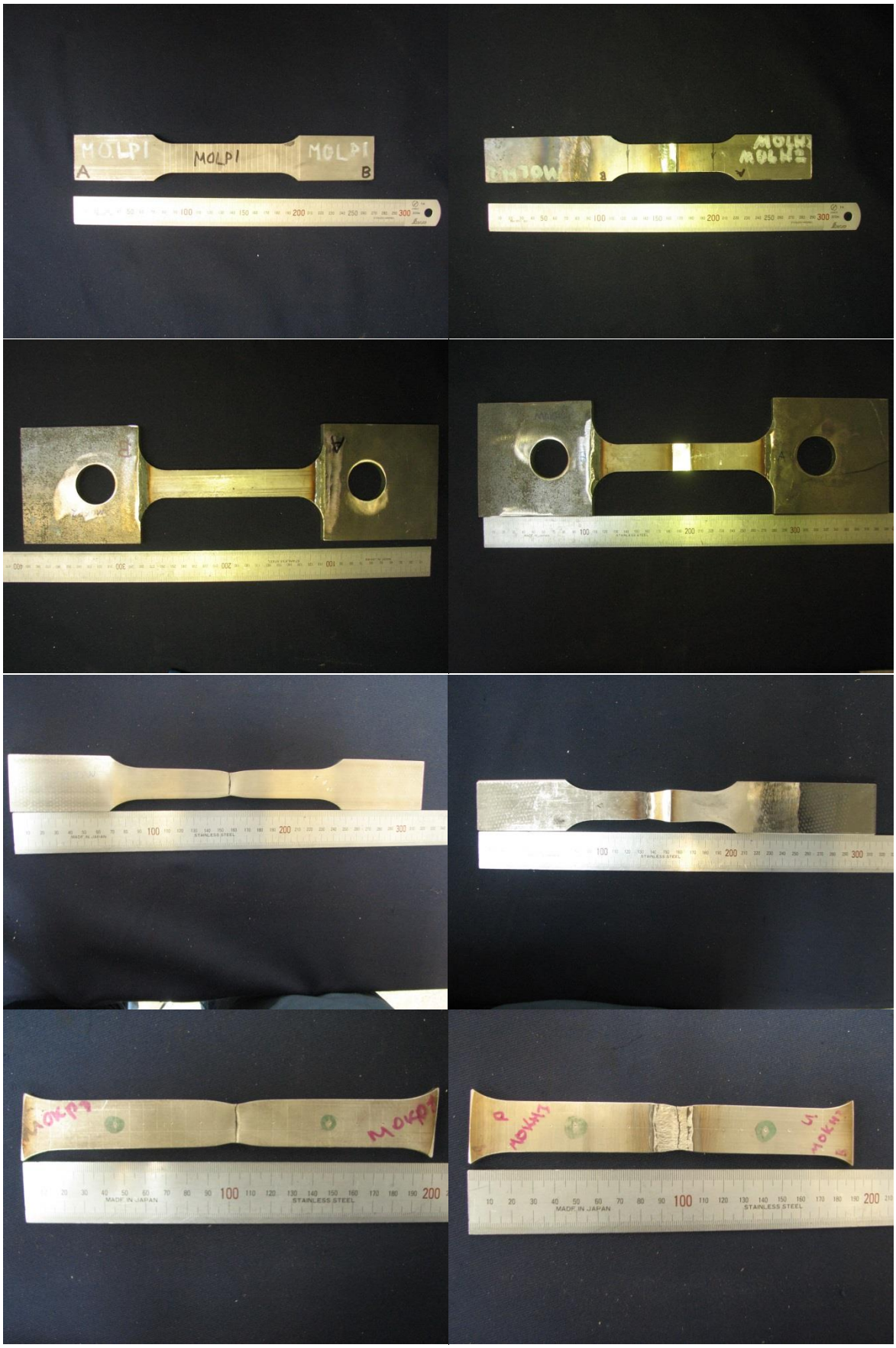
APPENDIX 4. Figures of the tensile test specimens.